Duch W, Tołpa K, Ratajczak E, Hajnowski M, Furman Ł, Alexandre L. (2023)
Asymptotic spatiotemporal averaging of the power of EEG signals for schizophrenia diagnostics.
Communications in Computer and Information Science (Springer Nature Singapore) 1963, pp. 428–439, 2024.

Presented at: ICONIP 2023, International Conference on Neural Information Processing, Changsha, China.
DOI: https://doi.org/10.1007/978-981-99-8138-0_34

# Asymptotic spatiotemporal averaging of the power of EEG signals for schizophrenia diagnostics

Włodzisław Duch[1] [0000-0001-7882-4729], Krzysztof Tołpa[1] [0000-0001-6223-234X], Ewa Ratajczak[2] [0000-0002-6628-1955], Marcin Hajnowski[2] [0000-0001-9109-760X], Łukasz Furman[1] [0000-0002-6960-8933], and Luís A. Alexandre[3] [0000-0002-5133-5025]

[1] Dept. of Informatics, Institute of Engineering and Technology, Faculty of Physics, Astronomy & Informatics, Nicolaus Copernicus University,
[2] Institute of Psychology, Faculty of Philosophy and Social Sciences, Nicolaus Copernicus University, Poland
[3] Universidade da Beira Interior, and NOVA LINCS, Covilhã, Portugal.

**Abstract.** Although many sophisticated EEG analysis methods have been developed, they are rarely used in clinical practice. Individual differences in brain bioelectrical activity are quite substantial, therefore simple methods that can provide stable results reflecting the basic characteristics of individual neurodynamics are very important. Here, we explore the potential for brain disorder classification based on patterns extracted from the asymptotic spatial power distributions, and compare it with 4-20 microstates, providing information about the dynamics of clustered global power patterns. Applied to the 16-channel EEG data such methods gave discrimination between adolescent schizophrenia patients and a healthy control group at the level of 86-100%.

**Keywords:** EEG, power spectra, STFT, microstates, neurodynamics, schizophrenia diagnostics, machine learning.

## 1 Introduction

Bioelectrical brain activity is frequently measured using electroencephalography (EEG) or magnetoencephalography (MEG). Such signals may have a high sampling rate, with temporal resolution below a millisecond. On the other hand, functional magnetic resonance (fMRI) measuring blood-oxygen-level dependent (BOLD) hemodynamic signals provides information about metabolic demands with a much lower temporal resolution of the order of one second. Both methods are used to diagnose mental disorders, neurofeedback, and many other applications.

Although many sophisticated approaches to EEG analysis have been developed, they are rarely used in clinical practice. Bioelectrical brain activity is non-stationary, even during short periods. Individual differences are quite large. Neurodynamics, especially in the resting state, strongly depends on hundreds of confounds [1]. Methods tested on a small number of samples give good results for favorably tuned parameters but in real life do not generalize well. Good biomarkers for objective diagnosis of brain disorders are still unknown [2]. Neural and genetic fingerprints of brain disorders may belong to

large clusters, reflecting the fundamental character of individual genetic or neurodynamic processes. Still, rare cases may be impossible to diagnose without similar patterns in the dataset used for training. Methods that reach 100% accuracy on small datasets have little chance of being useful.

EEG recordings involve a spatial distribution of power and temporal dynamics. The human brain contains about 2-4 million cortical columns, each containing tens of thousands of neurons, generating oscillations with frequencies reaching hundreds of hertz. EEG measurements are characterized by a spatial resolution of one centimeter and are usually analyzed in the 0-50 Hz range (intracranial iEEG may include 500 Hz ripples). The activity of large-scale neural networks can be used for biometric identification [3]. Specific patterns (fingerprints) of brain activity have diagnostic value. EEG recordings may detect the activity of more than ten large-scale networks linked to specific information processing (visual, auditory, sensorimotor, salience, dorsal and ventral attention, or default mode). This requires co-registration with the fMRI signal, which is technically very difficult [4].

In this paper, we have used a data-driven phenomenology that reflects the actual physiological processes. First, the limits of both spatial averaging of power in the narrow frequency bands and temporal characterization of brain processes using a large number of microstates, are explored. Tests were made on a typical, small EEG dataset of 45 schizophrenic adolescents [5]. Many papers were tested on even smaller EEG data, of 14 schizophrenia cases. Second, we investigate why several papers (see [6] and the review in [15]) can get 100% accuracy on such datasets. Classification may be successful if cases of similar structure are in the training set. Perfect classification accuracy is reached when features are selected on the whole data, before training a classifier (which is a common practice). Feature selection on the cross-validation training partition may lead to errors, identifying rare cases that should be inspected separately.

The methods applied in our study are described in the next section, followed by the description of the real data used for testing in the third section, and the results obtained in section four; the paper ends with the final discussion.

## 2 Methods

### 2.1 Microstates

EEG microstate analysis is a very popular method that may be used to generate features useful for classification. Global field potential (GFP) is calculated as the variance of potential $V_i(t)$ on the scalp:

$$GFP(t) = \sqrt{\frac{1}{N}\sum_{i=1}^{N}\left(V_i(t) - \bar{V}\right)^2}$$

Local maxima of GFP represent quasi-stable attractor states, transient activity patterns across all electrodes lasting from milliseconds to seconds. Such metastable field potential patterns are clustered for groups of subjects to identify classes of microstate

topologies. Two clusterization methods are most frequently used: the k-means approach and the "topographic atomize and agglomerate hierarchical clustering" (TAAHC, [7]). The whole time series is divided into windows assigned to a given microstate class based on the spatial similarity metric between each consecutive EEG sample and each microstate class. Initially, only four stable microstates were distinguished [8], and rarely more than ten classes were used for analysis.

Despite its great popularity, the microstate approach is burdened by some serious methodological limitations [9], drastically oversimplifying complex EEG signals. Ascribing various brain states to only a few clusters makes using statistical methods and symbolic dynamics techniques feasible, but a lot of information is lost. EEG oscillations show complex dynamics in different frequency bands between GFP peaks. Spatial power distribution patterns of microstates are too simple to accurately reflect the activity of large-scale brain networks.

We have performed MS analysis using the 'global maps strategy' [8-10] where one common set of *k* global maps is identified for all recordings, producing a set of common prototypes for both study groups. The analysis was carried out using freely available toolboxes for the MATLAB environment - the Microstate Toolbox EEGLAB plug-in [7] and the +microstate stand-alone package [11]. The initial steps included re-referencing to average reference and aggregating all EEG data fragments without normalization by average channel standard deviation. For each participant 1000 randomly selected EEG maps of the highest GFP at a minimum map distance of 10 ms were selected, discarding maps with GFP values exceeding one standard deviation of all maps' GFPs. Following normalization across the whole dataset, the selected maps were subjected to clustering using modified k-means (50 repetitions, 1000 maximum iterations, $10^{-6}$ threshold, cross-validation criterion measure of fitness). Maps were clustered selecting 4 to 20 microstate classes, and sorted by the global explained variance (GEV). Even number of microstate prototypes was used for microstate segmentation and backfitting to the data; sample maps were labeled based on the maximum similarity to the prototypes assessed with the global map dissimilarity (GMD) measure. The resulting microstate label syntax was subjected to temporal smoothing by rejecting small fragments below 30 ms. The following microstate statistics were calculated for each participant and used as features for classification: occurrence, duration, coverage, GEV, global field potential, mean spatial correlation, and the transition probabilities between microstate classes.

### 2.2 Spatial distribution of power

Our ToFFi toolbox for frequency-based fingerprinting of brain signals allows for the identification of specific frequencies ("fingerprints") arising in local brain regions, depending on the subnetwork that engages it in its activity [12]. Asymptotic average power distribution maps are more complex than MS maps and are good candidates for prototype states characterizing brain neurodynamics. To create such maps, we calculated short-time Fourier spectra (STFT) in 1-second sliding time windows. The STFT spectra were generated in windows starting in consecutive EEG samples, providing cumulative and average power estimations at discrete frequencies *f* for each electrode on

the scalp. Given a raw EEG data matrix $\mathbf{U}_k = (u_{ik}) = (u_k(t_i))$, where the index $i = 1..N$ enumerates time-series samples and index $k = 1..N_c$ refers to electrode number ($N_c$ data streams, input channels), the algorithm is summarized as follows:

- For each subject, given EEG data matrix $\mathbf{U}_k = (u_{ik})$
- Segment the data into time windows with $\tau$ samples, $\boldsymbol{w}_k(t_i) = [u_{ik}, u_{ik+\tau}]$.
- For each time window $i = 1..N-\tau$ calculate STFT power spectra $\boldsymbol{S}_k(t_i,f)$.
- Sum all $\boldsymbol{S}_k(t_i,f)$ over time windows to get local cumulative power $\boldsymbol{S}_k(f)$ in channel $k$ at frequency $f$.
- Calculate the average power $\boldsymbol{R}_k(f) = \boldsymbol{S}_k(f)/(N-\tau)$ in each channel.
- Sum $\boldsymbol{R}_k(f)$ over selected frequency ranges to estimate power in each band.

If the sampling frequency is high, windows may be shifted by several samples to speed up the calculations. This procedure creates for each subject a vector with the number of $N_c$ components estimating average power in different frequency ranges. We have found that these averages stabilize after about 60 seconds. Average power maps are relatively stable for each individual but do not contain any information about the dynamics or frequency. This kind of information may be added by dividing the whole frequency range of the STFT spectra into typical frequency bands (δ, θ, α, β, γ) or by focusing on several narrow few-Hz bands to capture power peaks that arise at the same time in several channels, reflecting synchronized processes.

The avPP analysis can be extended in many ways. The global EEG signal at a given time moment $\mathbf{P}_M(t)$ may be decomposed using the basis calculated by asymptotic spatial averaging. The cumulative average power values and variances were calculated separately for each electrode for the broadband spectrum (0.5-60 Hz). After calculation of the STFT spectra, it is trivial to calculate the average power for classical EEG bands: delta (0.5-4 Hz), theta (4-8 Hz), alpha (8-12 Hz), beta (12-30 Hz), gamma (30-60 Hz). This will create vectors with $5\times N_c$ components. We have also calculated power in a narrow 1Hz band to see which frequencies lead to the most characteristic patterns, creating vectors with $60\times N_c$ components. Attractor states may be defined by monitoring the time windows in which the power decreases below a certain threshold. We can combine that with our approach to recurrence quantification analysis [13], estimating distances to our asymptotic distributions instead of self-similarity. To capture the flexibility of brain subnetworks [14] we can look at various functional correlation measures and average them in longer recordings.

## 3 Dataset and related papers

Diagnosis of schizophrenia based on EEG has been a popular subject, with over 40 methods mentioned in the summary by Khare, Bajaj, and Acharya [15]. They have tested their SchizoNET approach on EEG recordings of 45 adolescent boys (10-14 years old) with schizophrenia (schizotypical and schizoaffective disorders), described in Borisov et al. paper [5]. The control group of similar age consisted of 39 healthy schoolboys. EEG recordings were made in a wakeful, relaxed state with the eyes closed,

using 16 electrodes placed in the standard 10–20 system at O1, O2, P3, P4, Pz, T5, T6, C3, C4, Cz, T3, T4, F3, F4, F7, and F8. The sampling rate was 128 Hz, and only artifact-free EEG segments of the recordings were used for analysis.

Analysis performed in the original paper [5] was based on the index of structural synchrony (ISS), the synchronization frequency between 120 pairs of electrodes during quasi-stationary segments of the EEG signals, free from random coincidences. Resulting graphs showing connections between pairs of electrodes with high ISS have a little chance of being stable. We have made a similar investigation and in each cross-validation fold such graphs differ significantly. The overall conclusion from this paper is that schizophrenics have less synchronicity between electrodes that are far apart, but more for electrodes that are adjacent.

This data has been analyzed in many other papers, therefore we have a comparison with different methods of analysis. Several convolutional neural networks were applied to this data. SchizoNET [15] combined the Margenau–Hill time-frequency distribution (MH-TFD) and convolutional neural network (CNN) with only five layers. The time-frequency amplitude is converted to two-dimensional plots and fed as an image to the CNN model. Using 5-fold cross-validation (5 CV) this model achieved a very high accuracy of 97.4%. Phang et al. [16] developed a deep convolutional neural network (CNN) framework for the classification of electroencephalogram (EEG)-derived brain connectome in schizophrenia. They have used a combination of 3 methods: connectivity features based on a vector autoregressive model, partial directed coherence, and complex network measures of network topology. Different fusion strategies with a parallel ensemble of 1D and 2D CNNs to integrate the features from various domains, and analysis of dynamic brain connectivity using the recurrent neural networks. In the 5×CV tests, their fusion-based models CNNs outperform the SVM classifier (90.4% accuracy), achieving the highest accuracy of 91.7±4.6%. These models use full connectivity matrices in 5 bands, requiring vectors with 1280 components, and the full fusion models use vectors with 2730 dimensions. Aslan and Akin [17] converted EEG signals to 2D images using continuous wavelet transform and trained VGG16 deep learning network architecture on such images. They created vectors from 5-second sequences, dimension 10240, and transformed them into $224 \times 224$ scalograms. They claim an accuracy of 98% but have used a single partition of 20-80%, so it cannot be compared to cross-validation. Shen and colleagues [7] used dynamic functional connectivity analysis and 3D deep convolutional neural networks. A time-frequency domain functional connectivity analysis was used to extract the features in the alpha band only with a cross-mutual information algorithm. This gave 97.7±1.2% accuracy and some differences between the connectivity of temporal lobe areas in both the right and left side of the brain, between the schizophrenia and control subjects.

All these results are almost perfect, but none of these methods have the chance to be useful in a clinical setting. First, the “black box” approach provides no insight into the brain processes that may characterize schizophrenia. Second, feature selection on the whole dataset leads to high accuracy that significantly drops when selection is done only on the training partition. This is illustrated below.

# 4 Results

## 4.1 CNN calculations.

We have tested a typical convolutional neural network, considering the data from each subject as an image. The images were created by building a $N_c \times N_c$ distance matrix from the $N_c$=16 channel data, where the ($i$,$j$) pixel represents distance $d(X_i, X_j)$. Here $X_i$ is a $N_c$-dimensional vector with the value of each EEG channel at time instant $i$=1,.., $N$, the number of EEG samples $N$=7680 (128Hz×60s), and the distance function was Euclidean. This matrix was subsampled to a final size of 240×240 pixels. An example of such a matrix can be seen in Fig. 1. Our CNN had 3 convolutional layers, with 16 3×3 filters in the first layer, 32 3×3 filters in the second and 64 3×3 filters in the third convolutional layer, a ReLU layer after all convolutional layers, and two fully connected maxpooling layers after the ReLU layers of the convolutional blocks. Batch normalization layers are after the second and third convolutional layers, the output layer is followed by softmax nodes, with a total of 945170 parameters. This network was trained with a dropout of 0.25 before the first fully connected layer, using the Adadelta optimizer, for 200 epochs, and the best cross-entropy validation loss weights were used for testing. No information about the test partition has been used at any stage of calculations.

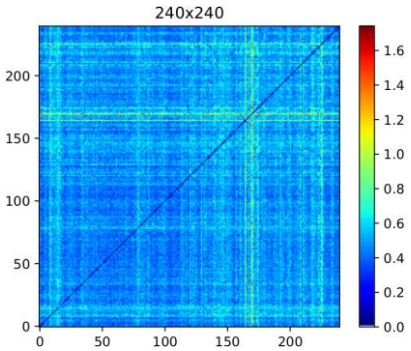


**Fig. 1.** An example of a subsampled distance matrix used in the experiments with CNNs.

5-fold cross-validation gave 79.8±5.9% average accuracy. This is more realistic than accuracies that are close to 100%. Such impressive results may come from a common error, performing feature selection on the whole dataset instead of only on the training partition within cross-validation folds. Sophisticated neural models can achieve high classification accuracy, but do not help to understand EEG data. The use of fMRI data for schizophrenia diagnosis seems to be about as accurate as EEG, for example, a model for automated schizophrenia diagnosis with fMRI features had accuracy below 80% in all cases [18]. Unfortunately, we do not have EEG and fMRI data for the same group of patients, therefore direct comparison of the two approaches is impossible.

Classification results presented below were made using the linear SVM method implemented in a Scikit-learn Python library, with the stratified 5-fold cross-validation. One advantage of such an approach is that the model is simple, and we can identify combinations of electrodes and frequency bands providing specific spatial information about localized oscillatory brain activity.

### 4.2 Microstate-based calculations

We have performed calculations with up to 20 microstates, generating features for the LSVM classifier. Detecting a large number of microstates should create smaller and more specific clusters. However, microstate algorithms cluster many states around the peak global power, so all maps resemble variations on similar patterns (Fig. 2). Additional microstates do not show complex patterns that could represent the activation of large-scale brain networks. The results of the classification are in Table 1 and Fig. 3.

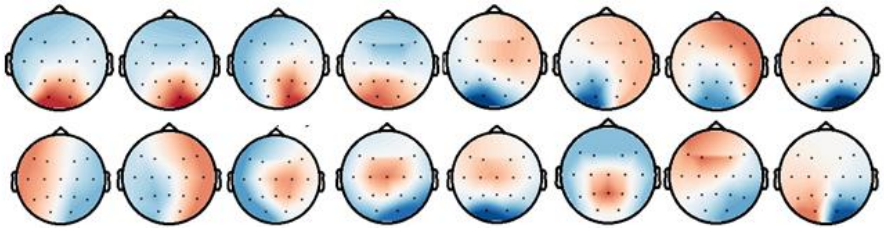

**Fig. 2.** Maps of 16 microstates classes from calculations on the whole dataset.

Results of classification based on 14 to 20 microstate features derived from the whole dataset were surprisingly high, reaching 100% in the 5-fold cross-validation. For these calculations, we used a common set of features selected before training the LSVM classifier on the whole dataset, using recursive feature elimination with cross-validation (RFECV). With a small dataset and a large number of parameters (the number of transition probabilities is equal to the square of the number of microstates), we can always find some parameters that distinguish a single case from all others. Feature selection within cross-validation done separately on the training partition will not discover such prominent features, and therefore untypical cases are misclassified.

Using a common set of features 100% accuracy is reached for 14 or more microstates, with the variance of results quickly decreasing to zero. Most useful features are based on transition probabilities (Fig. 4), showing the importance of dynamics. Performing feature selection within the training partition gives much worse results. Accuracy reaches 83.5±13,7% for 16 microstates, using 185 features. Almost as high accuracy 82.1±15.2% is reached for 12 microstates with only six features. Among the additional 179 features, some are useful only for a single, very specific case (a single test error contributes about 6% to accuracy). Cross-validation may put such cases in the test partition, leading to a large variation in the number of errors.

To find unusual cases in the schizophrenia dataset we have performed the leave-one-out tests, checking which cases/features are responsible for errors. For 16 microstates accuracy grows to 86.8%, with about 2-3 cases misclassified. Reliable classifiers should

estimate the confidence of their predictions distinguishing a group of typical cases for a given class and designating all others for more detailed evaluation.

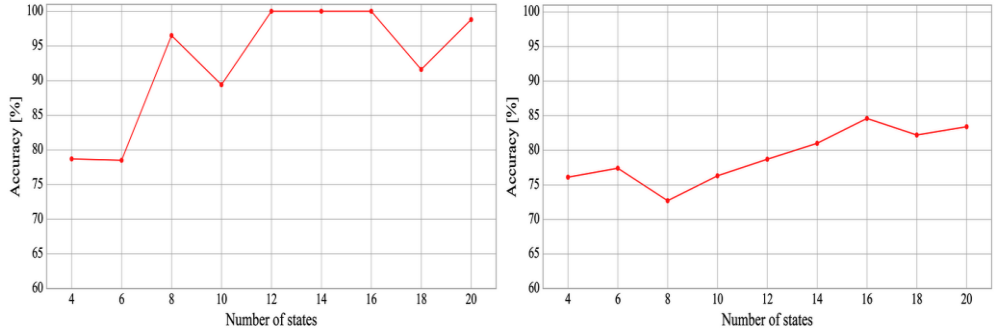


**Fig. 3.** 5×CV accuracy dependence on the number of microstates; left - recursive feature selection on all data; right - feature selection performed separately within each training fold.

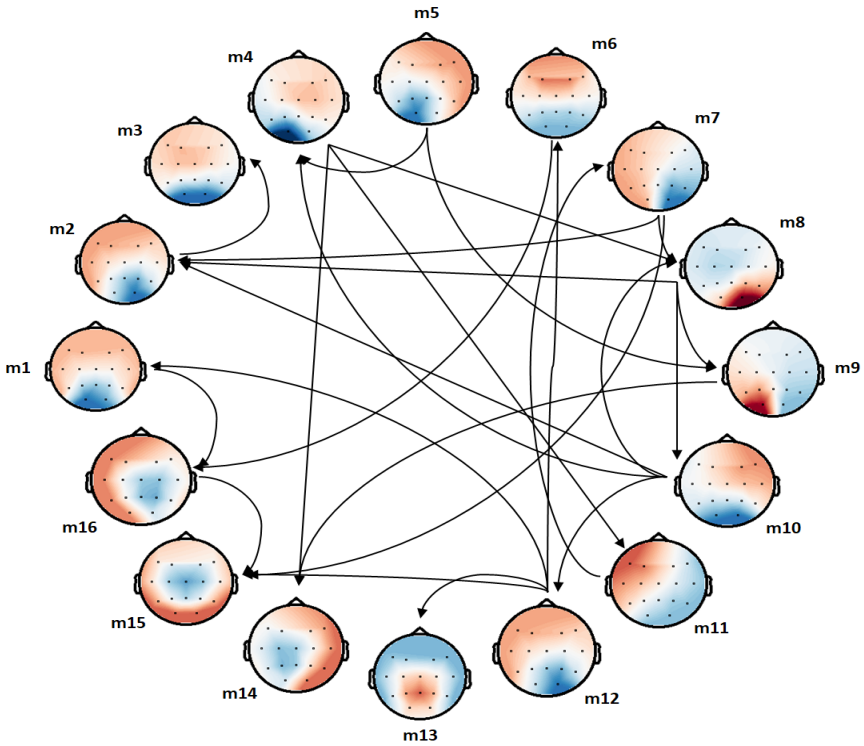


**Fig. 4.** Most important transition probabilities between 16 microstates used as features for the LSVM classifier that works with 100% accuracy.

| Microstates | | Selection on all data | | Selection on training only | | |
|---|---|---|---|---|---|---|
| N states | Type | N dim | Acc±Var % | Type | Ndim | Acc±Var % |
| 4 | TAAHC | 4 | 78.7±17.2 | TAAHC | 4 | 76.1±18.6 |
| 6 | TAAHC | 52 | 78.5±17.7 | TAAHC | 52 | 77.4±17.7 |
| 8 | TAAHC | 17 | 96.5±3.4 | TAAHC | 17 | 72.7±20.2 |
| 10 | TAAHC | 93 | 89.4±9.4 | TAAHC | 93 | 76.3±18.5 |
| 12 | K-means | 55 | **100** | K-means | 55 | 78.7±17.5 |
| 14 | K-means | 90 | **100** | K-means | 90 | 81.0±15.9 |
| 16 | TAAHC | 42 | **100** | K-means | 17 | **84.6**±13.0 |
| 18 | TAAHC | 281 | 91.6±7.8 | TAAHC | 281 | 82.2±14.0 |
| 20 | TAAHC | 221 | 98.8±1.2 | TAAHC | 221 | 83.4±14.3 |

**Table 1.** Classification results using parameters derived from microstates.

### 4.3 Asymptotic spatial power distribution

For the purpose of the classification, the last cumulative average power values (following the summation over the whole signal; in our case, 60 seconds) and the corresponding variances were used. They were normalized within the frequency range for each subject separately and used for the feature matrix. We have tested several combinations of feature sets, selecting values separately for different bands (see Table 2).

Additionally, to exclude irrelevant features, we have used a recursive feature elimination technique with 5-fold cross-validation taken from the Scikit-learn function. During cross-validation, the algorithm performs step-wise removal of data components based on the value of the SVM coefficients. We also present results obtained using recursive feature selection on the whole dataset and selection within the training partition in 5×CV.

A summary of the best classification results is presented in Table 2. The best results are obtained for the feature set consisting of cumulative average power values using the delta band in combination with theta, alpha, and gamma. Good results are also achieved for theta combined with beta bands taken together and reduced to 42 dimensions following the recursive feature elimination (RFECV).

Power plots in Fig. 5 are averaged over the five frequency bands. Power distribution patterns differ for each band and have a more complex structure than the microstates.

Compared to the control group, schizophrenia patients show larger regions of high activity, as well as lower activity in the left and higher in the right temporal lobe. This confirms the observations reported by Shen et al. [7]. The number of features was optimized and fixed for all folds, using the RFECV scikit function.

| EEG bands | Selection on all data | | Selection on training | |
|---|---|---|---|---|
| | N dim | Acc±Var % | N dim | Acc±Var % |
| broadband | 10 | 72.5±20.6 | 10 | 68.0±22.8 |
| β+γ | 3 | 73.8±19.6 | 3 | 72.7±20.5 |
| θ+β | 23 | 74.9±18.4 | 23 | 65.4±23.0 |
| δ+θ | 19 | 68.9±21.0 | 19 | 65.6±23.6 |
| δ+θ+α | 19 | 90.5±8.6 | 19 | 76.2±19.2 |
| δ+θ+α+β | 21 | **95.2±4.6** | 21 | 78.5±17.8 |
| δ+θ+α+β+γ | 71 | 79.5±15.5 | 71 | **79.8±17.1** |

**Table 2.** Summary of classification results for features obtained from asymptotic spatial averaging in selected bands. The window size was 256 samples.

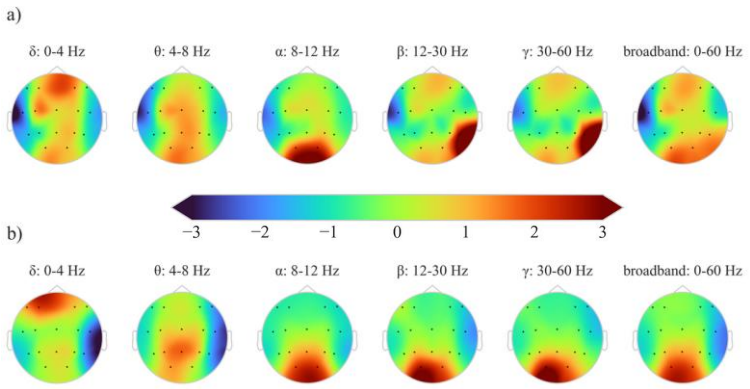


**Fig. 5.** Example of asymptotic power distributions. a) S27w1 schizophrenia, b)719w1 healthy.

The electrodes and frequency bands that contribute the most to the theta-beta SVM classification based on the maximum absolute values of the weights are shown below. Starting with the most important combinations, the top 10 include:

| | | | | | | | | | |
|---|---|---|---|---|---|---|---|---|---|
| T4 α | F8 α | P3 β | C3 β | O2 α | Pz α | F8 θ | P4 θ | T4 θ | T3 θ |

## 5 Discussion

The dynamics of the brain states is characterized by a sequence of metastable states. The key problem is to find the optimal complexity of representation, capturing sufficient information about spatial patterns and their dynamics. We have introduced here frequency-dependent asymptotic spatial averaging, creating reference patterns more complex than those provided by microstates. In our tests, these spatial states show high discriminatory power. Splitting and optimizing frequency bands, selecting channels/sources and specific bands, and adding statistical information about the dynamics of these states, in the same way as done in the microstate analysis, should improve the results further. Microstates maximize global explained variance, creating a few maps (usually 4 to 10). Michel and Koenig [9] have summarized microstate parameter changes (Dur, Occ, Cov, GEV) calculated for subjects suffering from neuropsychiatric diseases. This is very crude and not sufficient for precise diagnosis. Here, we have performed microstate analysis with up to 20 states, focusing on generating features useful for classification. Transition probabilities between microstates (Fig. 4) provide especially useful features. Selecting a subset of these features on the whole dataset gives a set of features that give 100% correct classification using linear SVM in 5-fold cross-validation. Although no information about the test partition is used in the classifier training, such selection strictly on the training data strongly influences the results even in the leave-one-out procedure.

Small EEG data can always contain a few unique cases. All papers should clearly state whether feature selection has been performed separately in each cross-validation partition, or on the whole data. Rahman and colleagues [19] proposed an approach for the analysis of a small complex fMRI data called MILC (Mutual Information Local to the whole Context). A self-supervised pre-training scheme captured potentially relevant information from large data sets. This approach is similar to foundational models, pre-trained on large datasets to enable context embedding and trained on the local data. We see a similar phenomenon here but lack sufficiently large EEG data collections to create such foundational models.

Recurrence analysis is very well suited to the analysis of time series. Further work is needed to understand the relationship between microstates, recurrence states and their transitions, spectral fingerprints, average power plots, decomposition of signals into template models, and flexibility of transitions between different large-scale network states, graphs of transitions between ROIs, motifs derived from hidden Markov models, and subnetworks. All these issues require deeper investigation.

**Acknowledgments.** This work was supported by the Polish National Science Center grant UMO-2016/20/W/NZ4/00354, and NOVA LINCS (UIDB/04516/2020) with the financial support of FCT.IP, Portugal.

## References


1. Van De Ville, D., Farouj, Y., Preti, M.G., Liégeois, R., Amico, E.: When makes you unique: Temporality of the human brain fingerprint. Science Advances 7, eabj0751 (2021).
2. Abi-Dargham, A., Moeller, S. J., Ali, F., et al. (2023). Candidate biomarkers in psychiatric disorders: state of the field. World Psychiatry 22, 236–262.
3. Finn, E.S., Shen, X., Scheinost, D., Rosenberg, M.D., Huang, J., Chun, M.M., Papademetris, X., Constable, R.T.: Functional connectome fingerprinting: identifying individuals using patterns of brain connectivity. Nat. Neurosci. 18, 1664–1671 (2015).
4. Abreu, R., Leal, A., Figueiredo, P.: EEG-Informed fMRI: A Review of Data Analysis Methods. Frontiers in Human Neuroscience. 12, 29 (2018).
5. Borisov, S. V., Kaplan, A. Ya., Gorbachevskaya, N. L., & Kozlova, I. A. (2005). Analysis of EEG Structural Synchrony in Adolescents with Schizophrenic Disorders. Human Physiology, 31(3), 255–261. https://doi.org/10.1007/s10747-005-0042-z
6. Shen, M., Wen, P., Song, B., Li, Y.: Automatic identification of schizophrenia based on EEG signals using dynamic functional connectivity analysis and 3D convolutional neural network. Computers in Biology and Medicine. 160, 107022 (2023).
7. Poulsen, A.T., Pedroni, A., Langer, N., Hansen, L.K.: Microstate EEGlab toolbox: An introductory guide. bioRxiv. 289850 (2018).
8. Michel, C.M., Koenig, T.: EEG microstates as a tool for studying the temporal dynamics of whole-brain neuronal networks: A review. NeuroImage. 180, 577–593 (2018).
9. Shaw, S.B., Dhindsa, K., Reilly, J.P., Becker, S.: Capturing the Forest but Missing the Trees: Microstates Inadequate for Characterizing Shorter-Scale EEG Dynamics. Neural Computation. 31, 2177–2211 (2019).
10. Khanna, A., Pascual-Leone, A., Farzan, F.: Reliability of Resting-State Microstate Features in Electroencephalography. PLOS ONE. 9, e114163 (2014).
11. Tait, L., Zhang, J.: +microstate: A MATLAB toolbox for brain microstate analysis in sensor and cortical EEG/MEG. NeuroImage. 258, 119346 (2022).
12. Komorowski, M.K., Rykaczewski, K., Piotrowski, T., Jurewicz, K., Wojciechowski, J., Keitel, A., Dreszer, J., Duch, W.: ToFFi – Toolbox for frequency-based fingerprinting of brain signals. Neurocomputing. 544, 126236 (2023).
13. Furman, Ł., Duch, W., Minati, L., Tołpa, K.: Short-time Fourier transform and embedding method for recurrence quantification analysis of EEG time series. Eur. Phys. J. Spec. Top. 232, 135–149 (2023). https://doi.org/10.1140/epjs/s11734-022-00683-7.
14. Chinichian, N., Kruschwitz, J. D., Reinhardt, P., Palm, M., Wellan, S. A., Erk, S., Heinz, A., Walter, H., & Veer, I. M. (2023). A fast and intuitive method for calculating dynamic network reconfiguration and node flexibility. Frontiers in Neuroscience, 17. 2023.1025428
15. Khare, S.K., Bajaj, V., Acharya, U.R.: SchizoNET: a robust and accurate Margenau–Hill time-frequency distribution based deep neural network model for schizophrenia detection using EEG signals. Physiol. Meas. 44, 035005 (2023).
16. Phang, C.-R., Noman, F., Hussain, H., Ting, C.-M., Ombao, H.: A Multi-Domain Connectome Convolutional Neural Network for Identifying Schizophrenia From EEG Connectivity Patterns. IEEE J Biomed Health Inform. 24, 1333–1343 (2020).
17. Aslan, Z., Akin, M.: A deep learning approach in automated detection of schizophrenia using scalogram images of EEG signals. Phys Eng Sci Med. 45, 83–96 (2022).
18. Ellis, C.A., Miller, R.L., Calhoun, V.D.: Towards greater neuroimaging classification transparency via the integration of explainability methods and confidence estimation approaches. Informatics in Medicine Unlocked. 37, 101176 (2023).
19. Rahman, M.M., Mahmood, U., Lewis, N., Gazula, H., Fedorov, A., Fu, Z., Calhoun, V.D., Plis, S.M.: Interpreting models interpreting brain dynamics. Sci Rep. 12, 12023 (2022).